Insulating Ferromagnetism in La$_4$Ba$_2$Cu$_2$O$_{10}$: An *Ab Initio* Wannier Function Analysis

Wei Ku, H. Rosner, W. E. Pickett, and R. T. Scalettar

Department of Physics, University of California, Davis, California 95616-8677
(Received 14 May 2002; published 30 September 2002)

Microscopic mechanisms of the puzzling insulating ferromagnetism of half-filled La$_4$Ba$_2$Cu$_2$O$_{10}$ are elucidated with energy-resolved Wannier states. The dominant magnetic coupling, revealed through evaluated parameters (t, U, and J), turns out to be the intersite direct exchange, a currently ignored mechanism that overwhelms the antiferromagnetic superexchange. By contrast, the isostructural Nd$_4$Ba$_2$Cu$_2$O$_{10}$ develops the observed antiferromagnetic order via its characteristics of a 1D chain. Surprisingly, the in-plane order of both cases is *not* controlled by coupling between nearest neighbors. An intriguing pressure-induced ferromagnetic to antiferromagnetic transition is predicted.

Unlike most half-filled cuprates that feature the antiferromagnetic (AF) ground state as expected from the Hubbard model, a few of the cuprates possess exceptional ferromagnetic (FM) order instead [1–3]. In particular, half-filled Cu-d orbitals in the "brown phase" La$_4$Ba$_2$Cu$_2$O$_{10}$ (La422) are found to align ferromagnetically below 5 K [1,2], in great contrast to the isostructural Nd$_4$Ba$_2$Cu$_2$O$_{10}$ (Nd422) that retains antiferromagnetism below 7.5 K [4–6]. Such an unusual insulating FM phase poses a great challenge to our *quantitative* theoretical understanding of microscopic mechanisms involved in real materials.

Up to now, there are only limited pioneering attempts at identifying the quantum processes responsible for this intriguing behavior of La422. With elaborate perturbation on a *multiband* Hubbard-like model [7], it is suggested that destructive interference of hopping paths (between 6th order and 8th order terms) may suppress AF coupling and give a small FM coupling along the z axis in a very narrow parameter range, while the Goodenough process [8] between nearest neighbors produces the in-plane FM order. (More recently, the possible "crude link" to "flat-band ferromagnetism" in the Hubbard model was also pointed out [9].) However, this description is not very satisfactory; besides the bothersome narrowness of the parameter range, the resulting strength of the FM coupling is too small to account for the experiments [1]. Furthermore, the assumption of FM coupling between the nearest neighbors in the plane is apparently in contradiction to the AF order in Nd422 [5].

From the theoretical point of view, descriptions of quantum magnetism have been given mainly via phenomenological models like the Stoner, Heisenberg, Hubbard, or other tight-binding models [8,10], with adjustable parameters to fit the experiments. These approaches, though intuitive and computationally manageable, lack the quantitative detail of the complex interactions that occur in real materials. Sometimes even the sign of spin-spin coupling is simply chosen to fit the observed magnetic order. On the other hand, a normal practice of more

quantitative *ab initio* approaches [11], involving comparing total energy corresponding to different magnetic orders within the density functional theory (DFT) [12], not only suffers from the uncertain quality of existing approximate energy functionals [12] for the very sensitive magnetic systems, but it also hides the microscopic processes in a black box. The development of a unified scheme that simultaneously gives intuitive microscopic insight and quantitative realism of the *ab initio* level is thus highly desired.

In this Letter, aiming to resolve specifically the microscopic mechanisms of the unusual insulating ferromagnetism in La422, we attempt the first step of one such ambitious scheme by evaluating parameters (t, U, and J) of the (reformulated) *ab initio* second quantized Hamiltonian in the basis of localized energy-resolved Wannier states (WSs) [13–17], constructed from all-electron DFT orbitals [12]. A clear picture of microscopic processes involved naturally emerges from these parameters and the spatial distribution of the WSs. The dominant mechanism turns out to be the intersite FM "direct exchange" [10] that is currently ignored in the microscopic studies of this system. This process, occurring mainly at the La and O sites, overwhelms the weak tendency toward AF order via Hubbard-type superexchange [18]. The same analysis is then applied to Nd422 and used to demonstrate its characteristics of the 1D AF chain, as experimentally observed [4,5]. Surprisingly, in both compounds, the dominant (FM) exchange is found *not* with the nearest neighbors (currently assumed), but with sites above/below them, which simultaneously generates the proper in-plane order. Finally, the crucial role of the "chemical" effect is illustrated with a numerical simulation of La422 "under pressure," which suggests an intriguing pressure-induced FM to AF transition.

In order to uncover the underlying many-body interactions responsible for the observed magnetic order, mapping the system onto a simplified effective model Hamiltonian [17,19] is avoided. Instead, attention is paid to the full *ab initio* Hamiltonian, *rigorously* reformulated

into a "fluctuation" form that explicitly utilizes DFT solutions [20] (without "double-counting"):

$$H = \varepsilon_{\bar{\mu}\bar{\alpha}} n_{\bar{\mu}\bar{\alpha}} - t_{\bar{\mu}\bar{\nu}} c^{+}_{\bar{\mu}\bar{\alpha}} c_{\bar{\nu}\bar{\alpha}} + U_{\bar{\mu}} \tilde{n}_{\bar{\mu}\uparrow} \tilde{n}_{\bar{\mu}\downarrow}$$
$$+ \tfrac{1}{2} C_{\bar{\mu}\bar{\nu}} \widetilde{\tilde{n}_{\bar{\mu}\bar{\alpha}}} \widetilde{n}_{\bar{\nu}\bar{\beta}} - J_{\bar{\mu}\bar{\nu}} (S_{\bar{\mu}} \cdot S_{\bar{\nu}} + \tfrac{1}{4} n_{\bar{\mu}\bar{\alpha}} n_{\bar{\nu}\bar{\beta}})$$
$$+ \text{ other } (c^{+}_{\bar{\mu}\bar{\alpha}} c_{\bar{\mu}'\bar{\alpha}})(c^{+}_{\bar{\nu}\bar{\beta}} c_{\bar{\nu}'\bar{\beta}}) + \text{constant terms}, \quad (1)$$

where summation over barred variables is understood and $\tilde{o} \equiv o - \langle o \rangle^{\text{DFT}}$ denotes fluctuation from the expectation value $\langle o \rangle^{\text{DFT}}$ of operator o within DFT. Notice that the direct exchange (the 5th term) that directly couples spins is omitted in all the existing Hubbard-model based analysis of La422 and turns out to play a crucial role.

Extraction of parameters of this full Hamiltonian via traditional constraint DFT calculations [17,19] is extremely complicated (if possible at all). Instead, "bare" parameters $t_{\mu\nu} \equiv -\langle\mu|h^{\text{DFT}} - v^{\text{xc}}|\nu\rangle(1 - \delta_{\mu\nu}) + J_{\mu\nu}\langle c^{+}_{\nu\bar{\beta}} c_{\mu\bar{\beta}}\rangle^{\text{DFT}} \sim -\langle\mu|h^{\text{DFT}}|\nu\rangle(1 - \delta_{\mu\nu})$, $J_{\mu\nu} \equiv \langle\mu\nu|v|\nu\mu\rangle(1 - \delta_{\mu\nu})$, and $U_{\mu} \equiv \langle\mu\mu|v|\mu\mu\rangle$ are *directly evaluated* on the basis of half-filled, low-energy, localized WSs that possess the spin moment. (h^{DFT}, v^{xc}, and v are the DFT Hamiltonian, exchange-correlation potential, and bare Coulomb interaction, respectively.) These parameters prove to be insightful to illustrate the insulating ferromagnetism of interest, as they control how electrons (and spins) interact with each other (in a many-body environment) in real materials. Now, since solving the multiband Eq. (1) currently remains an important and yet challenging task, we proceed by identifying two primary microscopic mechanisms that appear naturally in Eq. (1): Hubbard-type AF superexchange [18] and FM direct exchange [10] (between the WSs). Their strength can be estimated by summing *phenomenological* formulas: $J^{SX} \sim -4t_{ij}^{2}/W_{j}$ and $J^{DX} \sim J_{ij}/2$, respectively, over leading exchange paths, where i and j are site indices. Screening of the WS on-site repulsion (including competing intersite Coulomb interaction and virtual processes involving states of higher energy) is accounted for by the reduction $W_{j} = U_{j}/2$, which is consistent with the value needed to give the correct Mott-Hubbard gap in cuprates. Considering the intersite nature of the direct exchange, the factor in J^{DX} is reasonable [21]. Our conclusion on the insulating magnetism of La422 is not very sensitive to the size of this renormalization.

The employment of the WSs (or "molecular orbitals in crystal") [13–17], instead of other orthonormal complete sets, is strongly physically motivated. In addition to their full awareness of crystal and local symmetries [15], the constructed WSs are *the most localized within the subspace of low-energy excitation,* which facilitate a direct physical interpretation consistent with interacting localized spins. This "energy resolution" naturally follows the identity of the subspace spanned by our WSs and that by the *chosen* eigenstates of h^{DFT}. In addition, single-particle properties of these WSs —("self-interaction" [22] free) orbital energy $\varepsilon_{\mu\alpha} \equiv \langle\mu|h^{\text{DFT}} - v^{\text{xc}}|\mu\rangle - U_{\mu}\langle n_{\mu\alpha}\rangle^{\text{DFT}}$, occupation number, and spin-moment— are directly

translated with information from the DFT calculation and are known *before* solving the many-body Hamiltonian. Specifically for La422, we are thus able to focus only on the *half-filled* low-energy WSs corresponding to the *two* partially occupied bands across the Fermi energy, as other particle/hole states are of much higher energy and with zero spin moment. Furthermore, superexchange involving other states diminishes due to orthogonality between subspaces.

In this work, h^{DFT} is chosen via local density approximation (LDA) [23] for La422 and via LDA + U [24] for Nd422 (to split Nd f states and prevent them from incorrectly falling on the Fermi energy). Values of U and J (chosen to be 6.7 and 0.7 eV) in LDA + U are not crucial as long as f hybridization with the WSs is eliminated.

The WSs in unit cell R and orbital m are constructed by $|Rm\rangle \equiv |\bar{k}m\rangle e^{-i\bar{k}\cdot R}/\sqrt{N}$, where N is the number of discrete k points in reciprocal space, and $|km\rangle = |\psi_{k\bar{m}'}\rangle\langle\psi_{k\bar{m}'}|km\rangle$ (band-mixed Bloch state of crystal momentum k) is transformed from the all-electron [25] DFT eigenstate $|\psi_{km'}\rangle$ [26] of band index m', to facilitate maximum localization of the WSs, which in turn minimizes the number of non-negligible constants in Eq. (1). We follow the first step in Ref. [14] to calculate $\langle\psi_{km'}|km\rangle$ by projecting onto the *chosen subspace* of $|\psi_{km'}\rangle$ (belonging to the two partially occupied bands) narrow Gaussian states, $|g_{m}\rangle$, each centered at one of the main lobes of Cu-d contribution, followed by symmetric orthgonalization: $\langle\psi_{km'}|km\rangle = \langle\psi_{km'}|g_{\bar{m}''}\rangle M_{\bar{m}''m}$; $M^{-2}_{m''m} \equiv \langle g_{m''}|\psi_{k\bar{m}'}\rangle\langle\psi_{k\bar{m}'}|g_{m}\rangle$. Because of the concentrated contribution from Cu-d orbitals and the fact that there is only one low-energy WS per Cu site, the resulting WSs are practically the same as the maximally localized WSs obtained from iteration procedure [14]. While denser k sampling can slightly refine the shape of the resulting WSs, a $7 \times 7 \times 8$ lattice is good enough to give a reliable description, as the "aliasing" caused by the overlap of WS with itself due to periodicity is eliminated.

The resulting low-energy WSs of La422, each centered at one Cu site, are shown in Fig. 1, in which isosurfaces of $|\langle x|Rm\rangle|^{2}$ in real space x are plotted, along with the crystal structure. Notice that the "hybridization" between Cu-d, O-p, and La-d orbitals is naturally built into each WS; in the traditional atomic-orbital based analysis [17], such hybridization would require inclusion of complicated hopping and interaction between several orbitals from Cu, O, and La covering larger energy, which in turn obscures straightforward visualization of key physical processes. The antibonding nature of the Cu-d and O-p orbitals is also easily observed, as well as the fascinating "ring" structure at the La sites, which turns out to play an important role.

The spatial distribution of the WSs also reflects that of the spin density: $\langle x|\bar{R}\bar{m}\rangle\langle c^{+}_{\bar{R}\bar{m}\alpha} c_{\bar{R}'\bar{m}'\alpha}\rangle\langle\bar{R}'\bar{m}'|x\rangle \sim |\langle x|\bar{R}\bar{m}\rangle|^{2}\langle n_{\bar{R}\bar{m}\alpha}\rangle$ for localized WSs. We found $\sim 50\%$ of the spin moment at the Cu sites, with 10% at each O near Cu and 2% at each La; the last naturally accounts for the
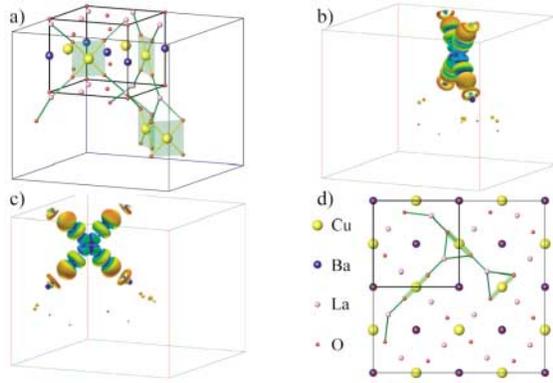
FIG. 1 (color). Crystal structure of La422 (a) and its top view (d) shown within $2 \times 2 \times 2$ unit cells. Most atoms outside the first unit cell are removed from panel (a) for clarity. (b),(c) Illustration of low-energy Wannier states with $R = (0, 0, 0)$.

experimentally observed hyperfine field for La [2]. Our WSs also illustrate, for the first time, the shape of the spin density at the La sites (as superposition of d orbitals of various symmetry), which has not been completely resolved by NMR measurement [2].

Figure 2 lists our calculated leading parameters. Note that $t_{Rm,R'm'} \sim \langle Rm|\bar{k}\bar{m}''\rangle \varepsilon_{\bar{k}\bar{m}''} \langle \bar{k}\bar{m}''|R'm'\rangle$ is easily *evaluated* with DFT eigenenergy $\varepsilon_{km''}$, in contrast to the conventional procedure of tight-binding *fit* [27]. (Since the resulting t_{ij} corresponds *exactly* to the original DFT eigenenergy, this can be viewed as a perfect "downfolding" [28].) U_i, and J_{ij} are obtained via careful numerical integration [20,29], instead of parametrized Slater integrals [30] that assume *atomic* orbitals with well-defined angular momentum. The resulting $U_i \sim 7.5$ eV is much smaller than that of atomic Cu-d orbitals, reflecting non-negligible hybridization (not delocalization).

The microscopic mechanisms for the unusual FM order are now easily visualized. Consistent with the extremely narrow bandwidth of the low-energy bands, hopping (t_{ij}) between the WSs is very small (Fig. 2), of a few meV, which brings about a weak AF tendency via superexchange [18]. Along the z axis (upper table), the FM direct exchange, commonly discarded in Hubbard-like models, clearly overwhelms the AF superexchange ($J_z^{DX} \gg$

J_z^{SX}). This process occurs mainly at the ring structure of WSs at the La sites (Fig. 1), where a large hyperfine field occurs [2]. In the language of atomic physics, this direct exchange is similar to what gives the first Hund's rule at La sites.

Interestingly, instead of the nearest neighbor interaction currently assumed, the in-plane FM coupling (middle table) turns out to be dominated by the (101) direct exchange (*above/below* the nearest neighbors), occurring mainly at O sites near Cu (Fig. 1.) Having the interplane FM alignment, a strong in-plane FM coupling is thus established, unchallenged by any AF coupling, due to zero hopping dictated by the local symmetry [15]. The resulting coupling constants are of the same order as the observed transition temperature (~ 5 K), which further rationalizes our phenomenological estimation.

For comparison, the AF order in Nd422 is also analyzed with the same technique. (According to the analysis of neutron diffraction measurement [5], the Nd moment is perpendicular to and "disconnected" from the Cu moment and thus is excluded in our analysis.) One immediately notices in Fig. 3 that the (001) hopping is considerably (~ 10 times) larger, which in turn greatly enhances the AF superexchange and thus allows it to overcome the (slightly enhanced) FM direct coupling along the z axis. Such strong 1D characteristics are in excellent agreement with the optical and neutron measurement [4,5]. In the xy plane, however, there exists *no* AF coupling between nearest neighbors but only FM exchange, primarily along (101), as in the case of La422. [The competing (100) FM coupling is weaker and connects to fewer neighbors.] We thus reach a surprising conclusion that, having the AF order between planes, *the observed in-plane AF order is actually caused by the (101) FM coupling.*

Insight into the dramatic difference in the z-axis hopping in these two compounds can be obtained by

i - j	(001)	(111)	(201)	(021)	$U_i = 7.49$ eV
t_{ij}	3.4	3.6	4.8	-0.10	$\left\lvert \mathcal{J}_z^{SX} = -0.11 \right\rvert$
J_{ij}	1.3	~0	~0	~0	$\left\lvert \mathcal{J}_z^{DX} \overset{\wedge}{=} 0.64 \right\rvert$
				(meV)	

i - j	(101)	(100)	
t_{ij}	0.0	0.0	$\left\lvert \mathcal{J}_x^{SX} = -0.0 \right\rvert$
J_{ij}	1.1	0.4	$\left\lvert \mathcal{J}_x^{DX} \overset{\wedge}{=} 1.27 \right\rvert$

i - j	(200)	(020)	(210)	(211)
t_{ij}	-8.8	0.71	±0.84	±0.64

FIG. 2 (color). Calculated parameters (in meV) for La422 and schematics of leading hopping (blue single arrows) and direct exchange (red double arrows) channels. Coordinate system for site indices i and j is defined for convenience.

i - j	(001)	(111)	(201)	(021)	$U_i = 6.12$ eV
t_{ij}	-31	7.8	8.0	-0.087	$\left\lvert \mathcal{J}_z^{SX} = -1.71 \right\rvert$
J_{ij}	2.1	~0	~0	~0	$\left\lvert \mathcal{J}_z^{DX} \overset{\vee}{=} +1.06 \right\rvert$
				(meV)	

i - j	(101)	(100)	
t_{ij}	0.0	0.0	$\left\lvert \mathcal{J}_x^{SX} = -0.0 \right\rvert$
J_{ij}	1.4	1.1	$\left\lvert \mathcal{J}_x^{DX} \overset{\wedge}{=} 0.87 \right\rvert$

i - j	(200)	(020)	(210)	(211)
t_{ij}	-1.7	1.1	±1.4	±0.38

FIG. 3 (color). Upper panel: calculated parameters (in meV) and schematics of Nd422 (cf. Fig. 2). Lower panel: comparison of WSs of Nd422, La422, and pressured La422.

comparing the corresponding WSs, shown in Fig. 3. In Nd422, the development of the extra p contribution (circled) at O sites that belong to the WS one layer below/above provides additional efficient hopping channels along the z axis. By contrast, the weak z-axis hopping in La422 is mainly through the (inefficient) ring structure at the La site and is further weakened by the residual hopping via O sites (not shown in Fig. 3), due to the phase difference between these two different routes. [This difference in hopping channels is clearly reflected in the sign of (001) hopping, since t_{ij}, unlike J_{ij}, is sensitive to the phase shift.] This weakening effect resembles the "interference" discussed in Ref. [7], except that in our analysis it is not responsible for the observed FM order.

The driving mechanism of this spatial redistribution of charge/spin is numerically examined by another set of calculations for La422 with lattice constants and atomic positions identical to Nd422 (La422 under pressure with $\sim 2\%$ reduction of the lattice constants). The resulting WSs, shown in Fig. 3, do not possess the extra O-p structure. Consistently, the key z-axis hopping reaches only 30% of that in Nd422 and the sign of (001) hopping remains positive. Evidently, the charge redistribution is mainly driven by the change of chemical environment surrounding Nd, which is smaller in size and consists of three f electrons and three more protons.

Intriguingly, while the resulting magnetic order remains FM, in good agreement with the experiment on La422 under pressure [6], moderate enhancement of t_{ij} and J_{ij} is observed due to slightly larger covalency, i.e., overlap between WSs. As a result, AF superexchange starts to approach the strength of the FM direct exchange (since t is squared) indicating a FM to AF transition upon *higher* pressure. We propose a further experiment with pressure slightly higher than 9 GPa to observe this fascinating FM to AF transition. Alternatively, this transition should be more easily achievable with moderate pressure on $(La_{0.8}Nd_{0.2})_4Ba_2Cu_2O_{10}$.

In summary, microscopic mechanisms of the puzzling insulating FM order observed in La422 are identified based on calculated parameters of interactions between half-filled localized WSs. The long-omitted FM direct exchange is shown to overwhelm AF superexchange. The spatial distribution of the constructed low-energy all-electron WSs provides detailed insight into the exchange processes and the partial contribution of spin moment, in agreement with the NMR measurement. The isostructural Nd422 is shown to possess characteristics of a 1D AF chain along the z axis, as experimentally observed, via extra efficient hopping through O sites. The in-plane magnetic order of both compounds turns out to be introduced via dominant FM coupling with (101) neighbors, not the nearest ones currently assumed. The crucial role of chemical replacement is illustrated via a numerical test on La422 under pressure, which further predicts an intriguing pressure-induced FM to AF transition. While future development for the many-body solution is desired,

our scheme already allows a detailed, quantitative, intuitive description of quantum magnetism that complements the common model approaches.

[1] F. Mizuno *et al.*, Nature (London) **345**, 788 (1990); H. Masuda *et al.*, Phys. Rev. B **43**, 7871 (1991).
[2] M. W. Pieper *et al.*, J. Magn. Magn. Mater. **135**, 319 (1994).
[3] L. J. de Jongh and A. R. Miedema, Adv. Phys. **23**, 1 (1974).
[4] I. V. Paukov *et al.*, Phys. Lett. A **157**, 306 (1991).
[5] I. V. Golosovsky *et al.*, Phys. Lett. A **182**, 161 (1993).
[6] H. Nozaki *et al.*, Phys. Rev. B **62**, 9555 (2000).
[7] S. Feldkemper *et al.*, Phys. Rev. B **52**, 313 (1995).
[8] J. B. Goodenough, J. Phys. Chem. Solids **287**, 6 (1958); J. Kanamori, *ibid.* **10**, 87 (1959); P. W. Anderson, Phys. Rev. **115**, 2 (1959).
[9] H. Tasaki, Prog. Theor. Phys. **99**, 489 (1998).
[10] J. E. Hirsch, Phys. Rev. B **59**, 436 (1999).
[11] V. Eyert *et al.*, Europhys. Lett. **31**, 385 (1995).
[12] W. Kohn and L. J. Sham, Phys. Rev. **140**, A1133 (1965).
[13] G. H. Wannier, Phys. Rev. **52**, 191 (1937).
[14] N. Marzari and D. Vanderbilt, Phys. Rev. B **56**, 12 847 (1997).
[15] V. P. Smirnov and D. E. Usvyat, Phys. Rev. B **64**, 245108 (2001).
[16] G. Berghold *et al.*, Phys. Rev. B **61**, 10 040 (2000); I. Schnell *et al.*, *ibid.* **65**, 075103 (2002).
[17] A. K. McMahan *et al.*, Phys. Rev. B **42**, 6268 (1990).
[18] P. W. Anderson, Phys. Rev. **79**, 350 (1950).
[19] M. S. Hybertsen *et al.*, Phys. Rev. B **39**, 9028 (1989).
[20] Wei Ku, W. E. Pickett, and R. T. Scalettar (to be published).
[21] This is different from the weak screening on *on-site intra-orbital* exchange in density-density interaction; D. van der Marel and G. A. Sawatzky, Phys. Rev. B **37**, 10674 (1988).
[22] J. P. Perdew and A. Zunger, Phys. Rev. B **23**, 5048 (1981).
[23] J. P. Perdew and Y. Wang, Phys. Rev. B **45**, 13 244 (1992).
[24] V. I. Anisimov *et al.*, Phys. Rev. B **48**, 16 929 (1993).
[25] Pseudopotential is avoided due to serious inaccuracy from lack of proper nodes in DFT orbitals. Wei Ku and A. G. Eguiluz, Phys. Rev. Lett. **89**, 126401 (2002).
[26] Evaluated with a full-potential LAPW code; P. Blaha *et al.*, computer code WIEN2K, Technical University of Vienna, 2001.
[27] D. A. Papaconstantopoulos and M. J. Mehl, Phys. Rev. B **64**, 172510 (2001), and references therein.
[28] O. K. Andersen *et al.*, cond-mat/0203083.
[29] The 6D integrations are evaluated accurately within atomic spheres [20], which should account for more than 90% of the contributions.
[30] J. C. Slater, *Quantum Theory of Atomic Stucture* (McGraw-Hill, New York, 1960), Vol. 1, p. 310.